Iterative technique for generating numerical on-axis holograms of an object on tilted planes using Rayleigh-Sommerfeld approximation

Técnica iterativa para la generación de hologramas numéricos sobre el eje de un objeto sobre planos inclinados utilizando la aproximación de Rayleigh-Sommerfeld

Roberto A Cuellar-Lozano[a]; **Jorge Enrique Rueda**[a];

[a] *Universidad de Pamplona, Colombia*

Correspondencia: roberto.cuellar@unipamplona.edu.co

Resumen

Presentamos una nueva técnica iterativa basada en la propagación sucesiva de campos utilizando la aproximación de Reyleigh-Sommerfeld (RS), para generar por computadora el holograma de amplitud en el eje de un objeto sobre un plano inclinado. La técnica fue validada realizando reconstrucción óptica y computacional del holograma.

Palabras clave: Holografía; Planos Inclinados; Hologramas Generados por Computador.

Abstract:

We present a new iterative technique based on successive field propagation using the Reyleigh-Sommerfeld (RS) approximation, to generate by computer the amplitude on-axis hologram of an object on a tilted plane. The technique was validated doing optical and computational reconstruction of the hologram.

Keywords: Holography; Tilted Planes; Computer Generated Holograms.

1 Introduction

Holography is a technique that allows the recording of the amplitude and phase of an object. To achieve this recording, two waves are needed, one reference and one object wave. The object wave refers to the reference wave diffracted by the object. [1] With the advance of the computers it was possible to carry out the calculation of the diffraction the plane objects using numerical techniques based on the scalar theory of diffraction. [2]

For years, the calculation of diffraction using numerical techniques was limited to objects on parallel planes. Leseberg and Frere propose a method for calculating Fresnel diffraction between tilted planes, using a Fourier transform, a coordinate transformation, and multiplying by a quadratic phase factor. [3] Matsushima et.al. propose a propagation method based on the angular spectrum and a rotation in the Fourier domain. [4] Chenliang et.al. use the fractional Fourier transform to calculate the propagation of an object on a tilted plane, after having performed a back-propagation of the previously rotated frequency domain. [5]

Other authors have been adding modifications to the method of coordinate rotation in the frequency domain. [6, 7] Jun Wu et.al. propose a method for calculating between tilted planes, using the non-uniform Fourier transform.[8]

In this paper we present an iterative technique based on successive field propagation in the Reyleigh-Sommerfeld regime for the construction of a virtual object on a non-tilted plane, of an object that lies on a tilted plane. Once the virtual object was built we generated its respective numerical on-axis hologram. Finally, we present results numerical and optical reconstruction of the hologram.
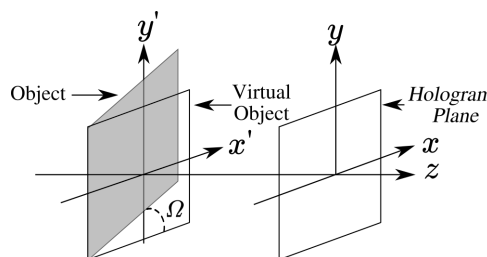
2 Method

Figure 1: Diffraction between tilted planes

It is well known that the field (U) diffracted by some object is a solution of the Helmholtz equation[1]:

$$(\nabla^2 + k^2)U = 0 \tag{1}$$

Different ways of solving this equation have been proposed, and each of them provides equivalent information in its spatial and frequency domains. The traditional way to solve the Eq.(1) is by using Green formalism, establishing boundary conditions on diffraction surfaces. The RS is the most general solution known. The solutions under the RS model are valid for propagation distances (z) from the object, greater than the wavelength (λ) of the incident wave. On the other hand, the solution using the angular spectrum (AS) constitutes a reasonably "simple" solution by propagating the U field as a linear combination of plane waves.

The two solutions mentioned (AS and RS) are equivalent, both representing the scalar field over $U(x,y,z)$ in terms of their boundary values in $U(x',y',0)$ over the plane (x',y') or over the frequency spectrum $\hat{U}(f_x, f_y, 0)$, where f_x, f_y spatial frequencies of these boundary conditions (fig.1). [9]

For the purpose of the present work, where we implement a technique of successive propagation from the near field, the representation of diffraction by means of the angular spectrum provides a significant advantage, this is because we can use the algorithm of the fast Fourier transform (FFT), so the computational speed of the method will be limited by the number of FFT required.

The angular spectrum of a field $U(x',y',0)$ on the plane (x',y') at a parallel plane (x,y) located at a distance z, is given by [10]:

$$U(x,y,z) \equiv P(U(x',y'),z) = ...$$
$$... = F^{-1}\left\{F\left\{U(x',y',0)\right\}H(f_x, f_y; z)\right\} \quad (2)$$

Where P corresponds to the AS propagation function, and the H free space transfer function is given by:

$$H(f_x, f_y; z) = \exp\left(\frac{2\pi z j}{\lambda}\sqrt{1 - (\lambda f_x)^2 - (\lambda f_y)^2}\right) \quad (3)$$

2.1 Geometric considerations of the method

In fig.2 there is a discretized object $t = t(m\delta x, n\delta y)$ of dimensions $L_X \times L_Y$, where $L_X = M\delta x$ and $L_Y = N\delta y$. t represents a transmittance matrix on some plane. Taking $m = 0, 1, ..., M-1$ y $n = 0, 1, ..., N-1$, then t will be expressed as:

$$t = t_{mn} \quad (4)$$

In this same fig.2 only the partitions on the axis x' are shown because the method was implemented for object plane inclined with respect to the axis x', as shown in (fig.1). In any case, the method can be applied for any other situation of a tilted of the object plane.

The method consists of 4 steps. The first one is to divide the entire horizontal dimension of t into D sections of specific range S_d. Step 2 consists in replacing such sections (S_d) in a three-dimensional array T(fig.2).

In the third step, iterative propagation is performed (fig.3). Finally, the hologram is calculated and digital or optical reconstruction is performed(fig.4).

2.2 Step 1

The array t is divided into D sections of range S_d along the x axis, naturally the division of M/D must result in an integer value, so the **first restriction**:

$$M \textbf{mod} D = 0 \quad (5)$$

Where **mod** refers to the M/D module. With the number of divisions D established, an array T of dimensions $M \times N \times D$ is defined. We will express each element of T as:

$$T = T_{mnd} = (W)_d, W \equiv T_{mn} \quad (6)$$

With this notation, $(W)_d$ represents the dth matrix $M \times N$ of the array T. The range S_d is established as a function of the value of D, L_x and d:

$$d\frac{L_X}{D} \leq S_d < (d+1)\frac{L_X}{D} \quad (7)$$
$$d = 0, ..., D-1$$

2.3 Step 2

Each substitution of the S sections of t is made on the corresponding S_d section of each matrix $(W)_d$, that is:

$$(W)_d = \begin{cases} t_{mn}, & \text{for } m \in S_d. \\ 1, & \text{otherwise.} \end{cases} \quad (8)$$

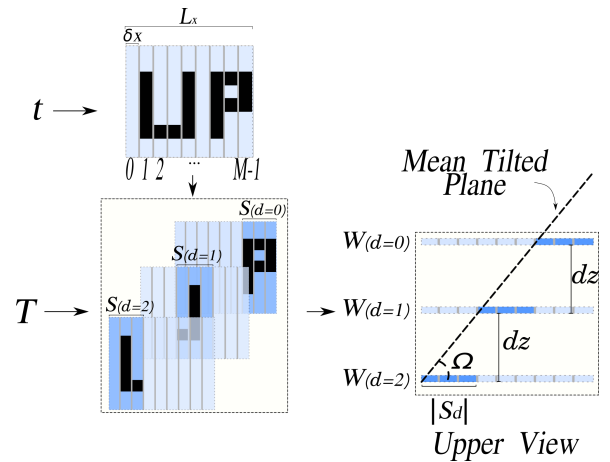In the fig.2 shows the replacement process for the case $M = 9$ and $D = 3$.

Figure 2: Arrangement T for the case $D = 3$

The value of $dz \to dz(M, D, \delta x, \Omega)$, corresponding to the separation between the *steps*, according to the fig.2 is:

$$dz = |S_d|\tan(\Omega) = \frac{\delta x M}{D}\tan(\Omega) \quad (9)$$

Here is the **second restriction** based on the scalar theory of diffraction in the RS regime, $dz >> \lambda$

2.4 Step 3

Once the constraints and geometric considerations of the model have been established, U_{-1} is defined as a constant amplitude reference plane wave, so that the propagation is direct and is governed under the following algorithm for case $D = 3$ (fig. 3):

1. Propagation of the object $U_0 = W_0 U_{-1}$ on the plane $d = 0$ at a distance dz, that is $P_0 = P(U_0, dz)$

2. Multiplication of $P_0 W_1 = U_1$ on the plane $d = 1$

3. Propagation of U_1 at a distance dz, that is: $P_1 = P(U_1, dz)$

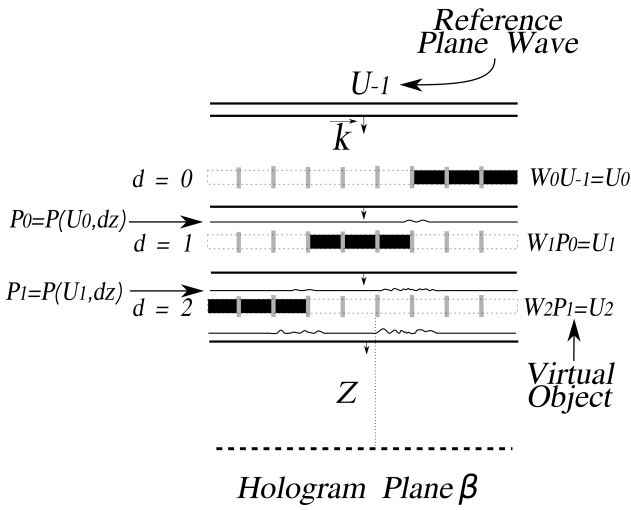4. Multiplication of $P_1 W_2 = U_2$ on the plane $d = 2$

Figure 3: Iterative propagation and hologram recording for the case $D = 3$

In the case $D = 3$, U_2 is defined as the virtual object. If we have D divisions, then $D - 1$ propagations must be made, then we can establish that the virtual object for $D = 3$ will be given by:

$$U_2 = P(U_1, dz)W_2 = P(P(U_0, dz)W_1, dz)W_2 = ...$$
$$... = P(P(U_{-1}W_0, dz)W_1, dz)W_2 \quad (10)$$

For the general case of D divisions, the virtual object will be:

$$U_{D-1} = P(U_{D-i}, dz)W_{D-1} \quad (11)$$

$$U_{D-i} = P(U_{D-i-1}, dz)W_{D-i}, \quad \text{for} \quad 2 \le i \le D \quad (12)$$

2.5 Step 4

Once you have the virtual object U_{D-1}, the hologram β (fig.3) on the axis is calculated at a distance Z from the virtual object:

$$\beta = |\beta_{D-1} + U_{-1}|^2, \; \beta_{D-1} \equiv P(U_{D-1}, \mathbf{Z}) \quad (13)$$

The computational reconstruction is performed in a similar way to the process of step in section 2.3. An array R of dimensions $M \times N$ is defined, as before, the elements of said array are defined as $R = R_{mn}$. The process is based on diffraction β, D times, and each of these diffractions is carried out at the distance corresponding to the position of each $(W)_d$ reconstruction subplanes (See section 2.3). In fig.4 the method of composition of the matrix R for any D is shown. The array R is composed as follows:

$$R_{mn} = |P(\beta, \mathbf{Z} + (D - 1 - d)dz)|_{mn}^2, \text{ for m} \in S_d \quad (14)$$
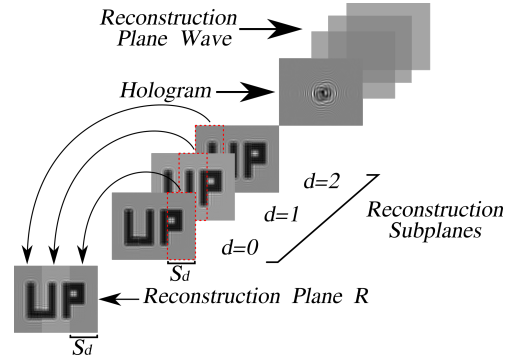

Figure 4: Reconstruction method.

3 Experiment and results

We developed an iterative algorithm to calculate the amplitude hologram of a two-dimensional image on a tilted plane. The virtual objects of the images in fig.5 and their respective holograms were calculated. Fig.6 shows the amplitude and phase of the virtual object calculated for the object of fig.5a, and its respective amplitude hologram (fig.6c). Fig.10 shows the computational reconstruction of the hologram shown in fig.6c.

Figure 5: Objects used. Object size: 60×40 pixels. Each object was embedded in an arrangement of size 1024×768 pixels.

The hologram reconstruction algorithm is applied independently to each section S_d, this is because each S_d corresponds to a reconstruction image plane located at a different Z.

On the other hand, the computational reconstruction of the hologram generates contrast breaks between the borders of neighboring reconstruction image planes (see fig.7a).

We eliminate the contrast breaks using an algorithm that calculates the average intensity (I_m) of each of the sections S_d in the reconstruction plane. Then, one of the values of I_m is taken as Offset, and this Offset is added or subtracted to the remaining sections S_d in the reconstruction plane (if Offset $> I_m$, then add Offset; if offset $< I_m$, then subtract Offset).
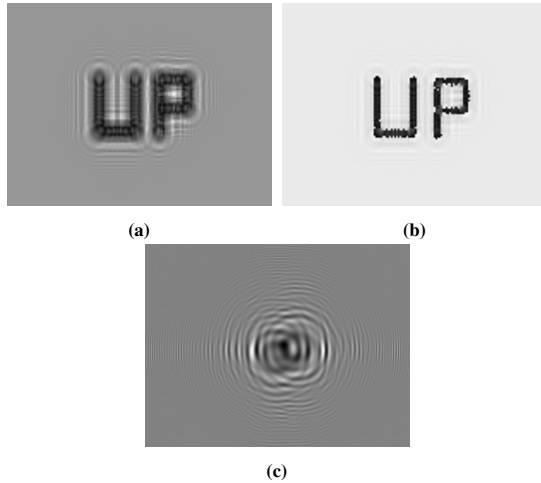
Fig.7 shows the computational reconstruction before and after correcting the contrast breaks. Fig.8 shows a profile of the reconstruction before and after correcting the contrast breaks. In the optical reconstruction no contrast breaks were observed (see fig.10).

A diagram of the experimental setup used for optical hologram reconstruction is shown in fig.9. This experimental arrangement was constructed using a He-Ne laser ($633nm$ wavelength), a spatial light modulator (LCR2500, dimensions: $1024(H) \times 768(V)$ pixels, pixel size $19 \times 19 \mu m$) and a video camera CMOS technology (dimensions: $2592(H) \times 1944(V)$ pixels, pixel size $2 \times 2 \mu m$). For more details of the optical elements used, see the references [11, 12].
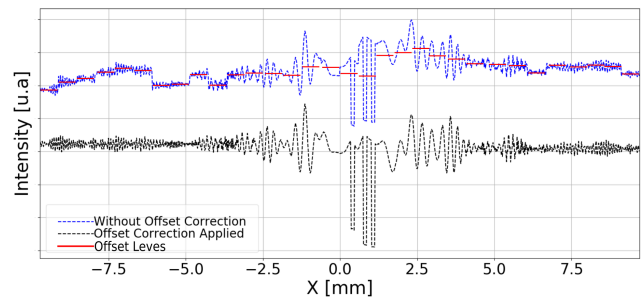

Figure 6: (a) Virtual Object Amplitude. (b) Virtual Object Phase. (c) Numerical on-axis hologram. Parameters used: $\delta x = 19 \mu m$, $D = 32$, $\lambda = 633nm$, $Z = 0.5m$, $\Omega = 28.5°$ and therefore $dz = 13.7 \mu m$

Figure 8: Correction of a profile of the reconstruction plane, before and after applying the *Offset*.
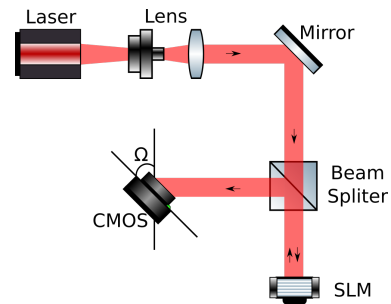

Figure 9: Experimental arrangement for optical reconstruction of the hologram on a tilted plane.

Fig.10 shows the computational reconstruction (fig.10a) and optics reconstruction (fig.10b).
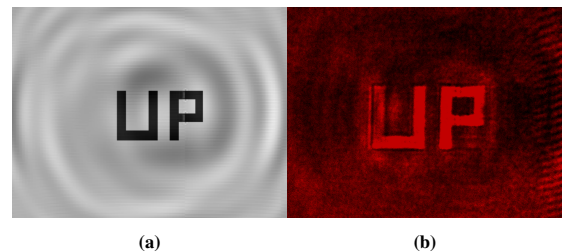

Figure 7: Computational reconstruction. (a) Reconstruction without offset correction. (b) Reconstruction with offset correction.

Figure 10: (a) Computational reconstruction. (b) Optical reconstruction. Parameters used: $\delta x = 19 \mu m$, $D = 128$, $\lambda = 633nm$, $Z = 0.5m$, $\Omega = 28.5°$ and therefore $dz = 13.7 \mu m$

In the case of the virtual object, of the object in fig.5b, in the reconstruction of its hologram, an optical test was performed to show the effect of angular non-focus $\Delta\Omega$ of the observation plane during the reconstruction of the hologram. Fig.12 shows an optical reconstruction sequence of the hologram. Fig.12a corresponds to an angular non-focus $\Delta\Omega = 35°$ and fig.12f corresponds to the focused observation plane ($\Delta\Omega = 0°$).
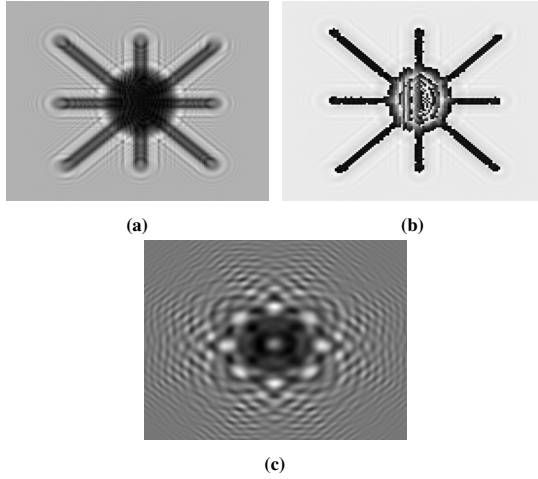

(a)   **(b)**

(c)

Figure 11: (a) Virtual Object Amplitude. (b) Virtual Object Phase. (c) Numerical on-axis hologram. Parameters used: $\delta x = 19\mu m$, $D = 128$, $\lambda = 633nm$, $Z = 0.5m$, $\Omega = 28.5°$ and therefore $dz = 13.7\mu m$

(a)   **(b)**
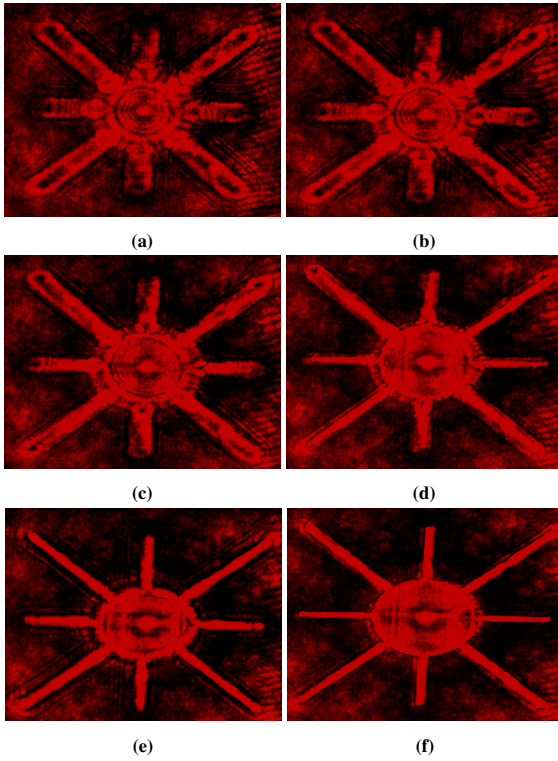
(c)   **(d)**

(e)   **(f)**

Figure 12: Optical reconstructions of the hologram on unfocused tilted planes to the tilted plane of correct focus. (a)$\Delta\Omega = 35°$. (b) $\Delta\Omega = 25°$. (c)$\Delta\Omega = 15°$. (d)$\Delta\Omega = 10°$. (e)$\Delta\Omega = 5°$. (f)$\Delta\Omega = 0°$

4 CONCLUSIONS

We proposed a new four-step holographic method to holographic image projection on tilted planes. Computationally on-axis amplitude holograms were generated. We developed an iterative algorithm of successive propagations, using the RS approximation to calculate the diffraction field on a $x'y'$ plane (virtual object) of the transmittance of an object on a tilted plane that have an angle Ω measured from the x' axis. The technique was validated by an optical and computational reconstruction of the hologram. We identified the origin of the contrast breaks in the numerically reconstructed image and proposed a correction method. We showed results of the tolerance to angular non-focus in optical reconstruction. An angular non-focus tolerance $< 5°$ was found (see fig.12). The computational cost of the technique is determined by the number of FFT operations η, that is $\eta\mathcal{O}(uMN(log(M) + log(N)))$, with u being a temporary variable.

References

[1] J. Goodman,Introduction to Fourier Optics (McGraw-Hill, USA, 1996).

[2] W. Jueptner and U. Schnars,Digital Holography (Springer, Germany, 2010).

[3] D. Leseberg and C. Frere, "Computer-Generated Holograms of 3-D Objects Composed of Tilted Planar Segments,"Appl.Opt27, 3020–3024 (1988).

[4] K. Matsushima, H.Schimmel, and F.Wyrowski, "Fast calculation method for optical diffraction on tilted planes byuse of the angular spectrum of plane waves," J.Opt.Soc.Am20(9), 1755–1762 (2003).

[5] C. Chang, J. Xia, and Y. Jiang, "Holographic image projection on tilted planes byphase-only computer generatedhologram using fractional fourier transformation," J. Disp. Technol.10, 107–113 (2014).

[6] S. D. Nicola, A. Finizio, G. Pierattini, P. Ferraro, and D. Alfieri, "Angular spectrum method with correction ofanamorphism for numerical reconstruction of digital holograms on tilted planes," Opt. Express13, 9935–9940(2005).

[7] W. Pan and Y. Zhu, "Fresnel diffraction method with object wave rotation for numerical reconstruction of digitalhologram on tilted plane," Optik124, 4328 – 4330 (2013).

[8] C. Chang, J. Xia, J. Wu, W. Lei, Y. Xie, M. Kang, and Q. Zhang, "Scaled diffraction calculation between tilted planesusing nonuniform fast fourier transform," Opt. Express22, 17331–17340 (2014).

[9] S. Orfanidis,Electromagnetic Waves and Antennas (Rutgers University, 2016).

[10] D. Voelz,Computational Fourier Optics: A MATLAB Tutorial(Spie Press, Bellingham, USA, 2011).

[11] D.Pabón, "Holografía digital objetos 3D, estudio e implementación de una interface óptico-digital para el registro-reconstrucción del holograma", Tesis de Maestría, Departamento de Física y Geología, Universidad de Pamplona, Pampona, 2012.

[12] D.Pabón, J.E Rueda, "Construcción de una interface óptico-digital para generar-reconstruir hologramas", Revista Colombiana de Tecnología de Avanzada, vol.1, no.21, pp.145-149.